Table V. Selected Bond Distances and Angles for $Fe_3(\mu_3\text{-PPh})(\mu_3\text{-PhPC\{OEt\}Ph})(CO)_9$ (16)

(a) Bond Distances (Å)			
Fe(1)-Fe(2)	2.671 (2)	Fe(1)-P(2)	2.240 (2)
Fe(1)-Fe(3)	2.750 (1)	Fe(2)-P(2)	2.211 (2)
Fe(2)-P(1)	2.198 (2)	Fe(3)-C(10)	2.139 (6)
Fe(1)-P(1)	2.256 (2)	P(2)-C(10)	1.800 (6)
Fe(3)-P(1)	2.192 (2)	O(10)-C(10)	1.447 (8)
(b) Bond Angles (deg)			
Fe(2)-Fe(1)-Fe(3)	90.3	Fe(2)-P(1)-Fe(3)	122.3 (1)
Fe(1)-P(2)-Fe(2)	73.7 (1)	Fe(2)-P(2)-C(10)	115.6 (2)
Fe(1)-P(1)-Fe(2)	73.7 (1)	Fe(1)-P(2)-C(10)	107.9 (2)
Fe(1)-P(1)-Fe(3)	76.4 (1)	Fe(3)-C(10)-P(2)	96.5 (3)

least-squares refinements and difference Fourier maps. In the final cycle, least-squares convergence was achieved upon refinement of the positional and anisotropic thermal parameters of all non-hydrogen atoms. A final difference Fourier map showed no unusual peaks; the highest peak of 0.74 e Å^{-3} was located midway between Fe(2) and Fe(3). Final positional parameters are listed in Table II, and relevant bond distances and angles are summarized in Table III.

X-ray Diffraction Study of $Fe_3(\mu_3\text{-PPh})(\mu_3\text{-PhPC\{OEt\}Ph})(CO)_9$ (16). A suitable crystal of **16** was obtained by recrystallization from hexane and was attached to a fine glass fiber with epoxy cement. Unit-cell dimensions were derived from the least-squares fit of the angular settings of 25 reflections, $20° \leq 2\theta \leq 30°$. A profile fitting procedure was applied to all intensity data to improve the precision of the measurement of weak reflections. Details of data collection, reduction, and refinement are listed in Table I.

No correction for absorption was applied to the intensity data due to the low absorption coefficient and regular crystal shape. The three Fe and two P atoms were located by direct methods (SOLV) with remaining non-hydrogen atoms located from subsequent difference Fourier syntheses. All non-hydrogen atoms were refined anisotropically. Hydrogen atoms were assigned idealized, updated locations (d(C-H) = 0.96 Å; $U = 1.2\ U_{iso}$ for the carbon atom to which it was attached). Phenyl carbons were fixed to fit rigid hexagons (d(C-C) = 1.395 Å). The final difference Fourier synthesis showed a disordered solvent molecule of low occupancy presumed to be hexane (maximum, 1.21 e/Å^3) which was not refined. An inspection of F_o vs. F_c values and trends based upon sin θ, Miller index, or parity group failed to reveal any systematic error in the data. All computer programs used in the collection and refinement of crystal data are contained in the Nicolet program packages P3, SHELXTL (version 5.1), and XFG. Atomic coordinates for **16** for the non-hydrogen atoms are provided in Table IV, and selected bond distances and angles are given in Table V.

Acknowledgment. We thank the Department of Energy, Office of Basic Energy Sciences, for supporting this research and the National Science Foundation for contributing funds toward the purchase of the X-ray diffractometer at the University of Delaware. G. Steinmetz and R. J. Hale of the Tennessee Eastman Co. are acknowledged for recording FD mass spectra.

Registry No. 1, 33519-79-8; **1**-d_{10}, 108034-84-0; **3**, 102-07-8; **3**-d_5, 108009-44-5; **3**-d_{10}, 108009-46-7; **4**, 94404-80-5; **5**, 94404-81-6; **6**, 94404-83-8; **6**-d_{15}, 108009-45-6; **7**, 94404-82-7; **8**, 108009-41-2; **9**, 94404-84-9; **9**-d_{15}, 108034-82-8; **10**, 6780-41-2; **10**-d_5, 108034-87-3; **10**-d_{10}, 108034-86-2; **11**, 108034-83-9; **11**-d_5, 108034-85-1; **12**, 93-98-1; **12**-d_5, 108034-88-4; **12**-d_{10}, 108009-47-8; **13**, 2603-10-3; **14**, 108009-42-3; **15**, 94404-85-0; **16** (isomer 1), 108009-43-4; **16** (isomer 2), 108101-11-7; $Li[HBEt_3]$, 22560-16-3; EtOTS, 383-63-1; [Cp2Fe][PF_6], 11077-24-0; *p*-tolylphenylurea, 4300-33-8; ethyl benzoate, 93-89-0.

Supplementary Material Available: Tables of atomic positional and thermal parameters and complete bond lengths and angles for **9** and **16** (8 pages); listings of structure factors for **9** and **16** (36 pages). Ordering information is given on any current masthead page.

Kinetic and Thermodynamic Acidity of Hydrido Transition-Metal Complexes. 4. Kinetic Acidities toward Aniline and Their Use in Identifying Proton-Transfer Mechanisms

Robin T. Edidin, Jeffrey M. Sullivan, and Jack R. Norton*

Contribution from the Department of Chemistry, Colorado State University, Fort Collins, Colorado 80523. *Received April 18, 1986*

Abstract: The kinetic deuterium isotope effects for $CpM(CO)_3H/CpM(CO)_3^-$ (M = Cr, Mo, W) self-exchange reactions in acetonitrile are consistent with a proton-transfer mechanism. The small counterion effect on the rate of self-exchange between $H_2Fe(CO)_4$ and $HFe(CO)_4^-$ is consistent with the absence of IR-observable contact ion pair formation by $[HFe(CO)_4]^-$. Brønsted plots (log of the rate constant vs. log of the equilibrium constant) are linear for proton transfers in acetonitrile from transition-metal hydrides to a series of para-substituted anilines. For $CpW(CO)_3H$ the Brønsted slope, α, is 0.65; for $HMn(CO)_5$ it is 0.54, for $H_2Fe(CO)_4$ it is 0.55, and for $HCo(CO)_4$ it is 0.48. The rates of proton transfer to aniline cover a range of 9 orders of magnitude for the transition-metal hydrides studied: from 1.0×10^{-3} M^{-1} s^{-1} for $HRe(CO)_5$ to 1.7×10^6 M^{-1} s^{-1} for $HCo(CO)_4$. These rates define a kinetic acidity series which for the most part parallels the thermodynamic acidities of these hydrides. This kinetic acidity series has been used to demonstrate that the reaction of $Cp_2Zr(CH_3)_2$ with $CpM(CO)_3H$ (M = Cr, Mo, W) occurs by a proton-transfer mechanism.

In 1982 we commented[1a] that "knowledge of proton-transfer rates (involving transition metals) in straightforward cases should help identify less obvious proton-transfer mechanisms." We then reported comparative rates in CH_3CN for proton transfers from $CpW(CO)_3H$ to $[CpW(CO)_3]^-$ and to morpholine and from $Os(CO)_4H_2$ to $[Os(CO)_4H]^-$ and to Et_3N; these results showed that, for a constant thermodynamic driving force, proton transfers to metal bases faced higher kinetic barriers than proton transfers to nitrogen bases. Pearson, Ford, and co-workers[2] have reported

(1) (a) Part 1: Jordan, R. F.; Norton, J. R. *J. Am. Chem. Soc.* **1982**, *104*, 1255. (b) Part 2: Jordan, R. F.; Norton, J. R. *Acs Symp. Ser.* **1982**, *No. 198*, 403. (c) Part 3: Moore, E. J.; Sullivan, J. M.; Norton, J. R. *J. Am. Chem. Soc.* **1986**, *108*, 2257.

(2) (a) Walker, H. W.; Kresge, C. T.; Pearson, R. G.; Ford, P. C. *J. Am. Chem. Soc.* **1979**, *101*, 7428. (b) Pearson, R. G.; Ford, P. C. *Comments Inorg. Chem.* **1982**, *1*, 279. (c) Walker, H. M.; Pearson, R. G.; Ford, P. C. *J. Am. Chem. Soc.* **1983**, *105*, 1179.

0002-7863/87/1509-3945$01.50/0 © 1987 American Chemical Society

that the deprotonation by methoxide ion of several transition-metal hydrides (mostly with the hydride ligands bridging two or more metals) in methanol is substantially slower than the deprotonation of nitrogen and oxygen acids with similar pK_a values. There appears to be a substantial barrier to the protonation and deprotonation of transition metals, much as there frequently is to protonation and deprotonation at carbon.

A useful tool for studying the deprotonation of carbon, nitrogen, and oxygen acids has been the construction of Brønsted plots (eq 1, where k is the rate constant for H^+ transfer and K is the

$$\log k = \alpha \log K + \text{constant} \quad (1)$$

equilibrium constant for H^+ transfer), which illustrate the variation in activation free energy $\Delta G^{\ddagger}$ with changes in the overall free energy of reaction $\Delta G°$.[3-8] The value of the Brønsted coefficient α depends on the size of the intrinsic barrier to proton transfer $\Delta G_0^{\ddagger}$ (the barrier when $\Delta G°$ is zero). If sufficiently large values of $\Delta G_0^{\ddagger}$ attend the deprotonation of all M–H bonds, α will not vary a great deal among their proton-transfer reactions, even ones with substantially different values of $\Delta G°$. The *relative* reactivities of transition-metal hydrides will then be approximately the same in all such reactions, and the relative rates of deprotonation of these hydrides by a standard base will define a relative kinetic acidity series which will be substantially duplicated in other reactions of these hydrides which proceed by proton-transfer mechanisms.

Of course we must be sure that our *apparent* proton-transfer reactions actually occur by proton-transfer mechanisms. Earlier[1a,b] we noted the possibility that these reactions might occur by rate-determining *electron* transfer, followed by fast hydrogen atom transfer. This possibility seemed most likely with self-exchange reactions such as reaction 2, where one-electron oxidation and

$$M{-}H + M^- \xrightarrow[\text{electron transfer}]{\text{rate-determining}} M{-}H^{\bullet -} + {}^{\bullet}M \xrightarrow[\text{atom transfer}]{\text{fast hydrogen}} M^- + H{-}M \quad (2)$$

reduction of both species should be facile. Our earlier observation[1a,b] of an anomalously high (i.e., less negative) $\Delta S^{\ddagger}$ for proton transfer in the $HCr(CO)_3Cp/Cr(CO)_3Cp^-$ system also suggested that the apparent proton transfer in that system might be occurring by a different mechanism.

We have therefore investigated the kinetic isotope effect on self-exchange reactions in the group 6 series $(CpM(CO)_3^-/CpM(CO)_3H$ for M = Cr, Mo, or W). We have also examined the variation of proton-transfer rate with thermodynamic driving force for a series of substituted anilines and have constructed Brønsted plots for $CpW(CO)_3H$, $HMn(CO)_5$, $H_2Fe(CO)_4$, and $HCo(CO)_4$. We have constructed a kinetic acidity series (relative rates of proton transfer onto the standard base aniline) which we believe can be used for the identification of proton-transfer mechanisms involving transition-metal hydrides. Finally, we have used this kinetic acidity series to demonstrate that the reaction of Cp_2ZrMe_2 with $HM(CO)_3Cp$ (M = Cr, Mo, W)[9] occurs by a proton-transfer mechanism.

Results

We have carefully measured the second-order rate constants k_{self}, activation parameters, and kinetic isotope effects for H^+/D^+ transfer in the $CpM(CO)_3H/CpM(CO)_3^-$ self-exchange series (M = Cr, Mo, W). The results, given in Table I, are similar for all three systems. (Although the individual rates in the $HCr/^-Cr$ system do not differ much from those we previously measured,[1a,b] collectively these more accurate data revise $\Delta S^{\ddagger}$ down into the range generally observed for proton-transfer reaction of metal hydrides.) The observed isotope effects are low in comparison with the isotope effects observed for carbon acids but are almost exactly those expected for metal acids. If we assume a symmetric linear M···H···M transition state with a decomposition mode replacing the initial M–H stretching vibration, the isotope effect for these self-exchange reactions should be given by eq 3.[10] If

$$\frac{k^{H}_{self}}{k^{D}_{self}} = \exp\left(\frac{hc[\nu(M{-}H) - \nu(M{-}D)]}{2kT}\right) \quad (3)$$

one takes ν(Mo–H) as 1790 cm^{-1} and ν(Mo–D) as 1285 cm^{-1},[11] the calculated k_H/k_D is 3.38; a ν(W–H) of 1845 cm^{-1} and a ν(W–D) of 1322 cm^{-1} [11] give a calculated k_H/k_D of 3.53; a ν(Cr–H) of 1765 cm^{-1} and a ν(Cr–D) of 1260 cm^{-1} give a calculated k_H/k_D of 3.39.

The agreement of the observed and calculated isotope effects argues that self-exchange proceeds either by rate-determining proton transfer or by rate-determining hydrogen atom transfer, and the former is much more likely. If proton transfer rather than electron transfer is rate-determining for the reaction of neutral metal hydrides with their anionic conjugate bases, the same is surely true for the reaction of neutral metal hydrides with neutral nitrogen bases. In the remainder of this paper we will assume proton-transfer mechanisms for reactions of both types.

One of the reasons we have chosen acetonitrile as our solvent for these studies is its effective solvation of cations, which discourages the formation of ion pairs.[1,12] Neither we[1] nor others[13] have seen IR evidence for contact ion pair formation between any

Table I. Kinetic Deuterium Isotope Effects for $CpM(CO)_3H/[CpM(CO)_3]K$ (M = Cr, Mo, W) Self-Exchange in Acetonitrile at 25 °C

MH or MD	$10^{-2}k_{self}$,[a,b] M^{-1} s^{-1}	kinetic isotope effect[b]	$\Delta H^{\ddagger}$,[b] kcal mol^{-1}	$\Delta S^{\ddagger}$,[b] eu
$CpCr(CO)_3H$	180 (10)		4.9 (2)	−22.6 (8)
		3.6 (2)		
$CpCr(CO)_3D$	50 (4)		6.4 (3)	−20.0 (8)
$CpMo(CO)_3H$	25 (2)		5.3 (3)	−25.3 (12)
		3.7 (2)		
$CpMo(CO)_3D$	6.7 (7)		6.3 (5)	−24.0 (8)
$CpW(CO)_3H$	6.5 (2)		5.2 (3)	−28.0 (9)
		3.7 (2)		
$CpW(CO)_3D$	1.7 (1)		6.2 (3)	−27.4 (9)

[a] The second-order rate constant k_{self} for H^+ transfer is the average of the value obtained by observing the Cp line width of M^- in the presence of MH and the value obtained by observing the Cp line width of MH in the presence of M^-, k_{self} for D^+ transfer has been corrected for incomplete D incorporation according to eq 26. [b] Numbers in parentheses are the estimated standard deviations in the least significant figure.

Table II. Counterion Effect on Rate of Proton Transfer in Acetonitrile at 25 °C

MH	base	$10^{-3}k_{self}$,[a] M^{-1} s^{-1}	$\Delta H^{\ddagger}$,[a] kcal mol^{-1}	$\Delta S^{\ddagger}$,[a] eu
$(CO)_4FeH_2$	$[(CO)_4FeH]PPN$	4.2 (4)	4.9 (2)	−25.5 (10)
$(CO)_4FeH_2$	$[(CO)_4FeH]K$	1.4 (2)	4.7 (1)	−28.6 (4)
$(CO)_4FeH_2$	$[(CO)_4FeH]Na$	1.2 (2)	4.5 (1)	−29.2 (5)

[a] Numbers in parentheses are the estimated standard deviations in the least significant figure.

(3) (a) Marcus, R. A. *J. Phys. Chem.* **1968**, *72*, 891. (b) Cohen, A. O.; Marcus, R. A. *Ibid.* **1968**, *72*, 4249.
(4) Kresge, A. J. *Chem. Soc. Rev.* **1973**, *2*, 475.
(5) Bell, R. P. *The Proton in Chemistry*; Cornell University Press: Ithaca, NY, 1973.
(6) Caldin, E., Gold, V., Eds.; *Proton Transfer Reactions*; Wiley: New York, 1975.
(7) Simmons, E. L. *Prog. React. Kinet.* **1977**, *8*, 161.
(8) Albery, W. J. *Annu. Rev. Phys. Chem.* **1980**, *31*, 227.
(9) (a) Renaut, P.; Tainturier, G.; Gautheron, B. *J. Organomet. Chem.* **1978**, *150*, C9. (b) Marsella, J. A.; Huffman, J. C.; Caulton, K. G.; Longato, B.; Norton, J. R. *J. Am. Chem. Soc.* **1982**, *104*, 6360. (c) Longato, B.; Martin, B. D.; Norton, J. R.; Anderson, O. P. *Inorg. Chem.* **1985**, *24*, 1389.
(10) Melander, L.; Saunders, W. H., Jr. *Reaction Rates of Isotopic Molecules*; Wiley-Interscience: New York, 1980; p 26.
(11) Davison, A.; McCleverty, J. A.; Wilkinson, G. *J. Chem. Soc.* **1963**, 1133.
(12) Coetzee, J. F. *Prog. Phys. Org. Chem.* **1967**, *4*, 45.
(13) Darensbourg, M. Y.; Jimenez, P.; Sackett, J. R.; Hanckel, J. M.; Kump, R. L. *J. Am. Chem. Soc.* **1982**, *104*, 1521 and references therein.

carbonylmetalate ion and Na^+, K^+, or PPN^+ (bis(triphenylphosphine)nitrogen(1+) cation)[14] in CH_3CN. As the nucleophilicity of carbonylmetalate anions decreases considerably with the formation of contact ion pairs,[13] one would expect k_{self} to decrease considerably in the presence of such ion pairs. We have checked the dependence of k_{self} for $H_2Fe(CO)_4/HFe(CO)_4^-$ on the nature of the counterion (Table II). The small effect observed is consistent with negligible contact ion pair formation by $HFe(CO)_4^-$ in acetonitrile and probably arises from minor differences among the counterions in the extent of formation of solvent-separated ion pairs (which would not be detected by IR).

We have chosen aniline as our standard base for measuring the relative kinetic acidities of transition-metal hydrides because of its advantages for NMR rate measurement. In most cases its equilibrium extent of deprotonation and formation of $PhNH_3^+$ is small, which is advantageous because the concentration of free base ([B]) can be set equal to the concentration of aniline added and is therefore accurately known.

If the extent of deprotonation is small, use of a base such as pyridine, with no other protons on the nitrogen, gives a weighted average chemical shift (eq 4) for the HM/pyH^+ protons which

$$py + H\text{-}M \underset{}{\overset{k_{H^+}(py)}{\rightleftharpoons}} pyH^+ + M^- \qquad (4)$$

weighted average chemical shift of transferred proton about that of H-M

is very close to that of the H–M protons. Thus little or no broadening of the H–M ^1H NMR resonance can occur before it coalesces into the weighted average HM/pyH^+ resonance, and it is difficult or impossible to obtain $k_{H^+}(py)$ from the H–M ^1H NMR line width.

In contrast, the extremely fast[15,16] rate of proton exchange between $PhNH_2$ and $PhNH_3^+$ (eq 5) means that the protons

$$PhNH_2 + \overset{+}{PhNH_3} \overset{fast}{\rightleftharpoons} \overset{+}{PhNH_3} + PhNH_2 \qquad (5)$$

removed from H–M by aniline are rapidly averaged with a large number of other protons before returning to H–M.[17] The weighted average chemical shift for the $H\text{-}M/PhNH_3^+/PhNH_2$ protons is thus (as illustrated in eq 6) far removed from that of

$$PhNH_2 + H\text{-}M \overset{k_{H^+}}{\rightleftharpoons} \overset{+}{PhNH_3} + M^- \qquad (6)$$

weighted average chemical shift of transferred proton far from that of H-M—approaching that of $PhNH_2$

the H–M protons regardless of the position of the deprotonation equilibrium. Thus the H–M ^1H NMR resonance can undergo substantial broadening before it coalesces into the weighted average resonance, and k_{H^+} is easily obtained from the increase in the H–M ^1H NMR line width produced by the addition of aniline. The line width of the ^1H NMR resonances of H–M always varies linearly with $[PhNH_2]$.

(14) Contact ion pair formation in CH_3CN has been reported between $Co(CO)_4^-$ and Tl^+: Schramm, C.; Zink, J. I. *J. Am. Chem. Soc.* **1979**, *101*, 4554.

(15) The rate constant for proton transfer between $PhNH_2$ and $PhNH_3^+$ is at least 10^8 M^{-1} s^{-1} at 25 °C: (a) Rate constants for thermoneutral proton transfer between nitrogens are nearly as large as those for exergonic proton transfers: Perrin, C. L.; Wang, W. *J. Am. Chem. Soc.* **1982**, *104*, 2325. (b) Proton transfer in CH_3CN between picric acid and methyl red (both of which have, in their protonated forms, pK_a values close to that[16] of anilinium) occurs with a 25 °C rate constant of 8×10^8 M^{-1} s^{-1}: Strohbusch, F.; Marshall, D. B.; Eyring, E. M. *J. Phys. Chem.* **1978**, *82*, 2447.

(16) Kolthoff, I. M.; Chantooni, M. K., Jr.; Bhowmik, S. *J. Am. Chem. Soc.* **1968**, *90*, 23.

(17) The back reaction ($M^- + PhNH_3^+ \rightarrow H\text{-}M + PhNH_2$) rate constants calculated from the data in Table V are at most, for the least acidic hydrides, 10^9 M^{-1} s^{-1}—roughly comparable to the rate constants for $PhNH_2/PhNH_3^+$ proton exchange.[15] However, these hydrides undergo little equilibrium deprotonation by $PhNH_2$ in a kinetic acidity experiment, so $[PhNH_2] \gg [M^-]$; thus $PhNH_3^+$ reacts much faster by reaction 5 than by reaction 6.

Table III. Thermodynamic Acidity (pK_a) of Substituted Anilinium Perchlorates in CH_3CN

aniline	pK_a	aniline	pK_a
4-methoxyaniline	11.3 (1)	4-iodoaniline	9.5 (1)
4-methylaniline	11.1 (1)[a]	4-(trifluoromethyl)aniline	8.6 (1)
4-fluoroaniline	10.7 (1)	ethyl 4-aminobenzoate	8.2 (1)
aniline	10.5 (1)[a]	2,4-dichloroaniline	8.0 (1)
4-bromoaniline	9.6 (1)	4-cyanoaniline	7.6 (1)

[a] Values determined elsewhere[12] and redetermined in this work. [b] Numbers in parentheses are the estimated standard deviations in the least significant figure.

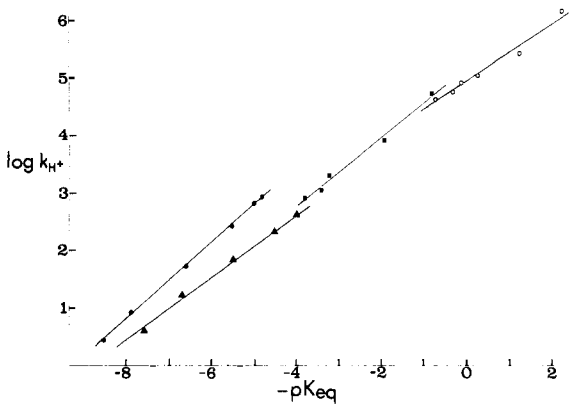

Figure 1. Plots of log k_{H^+} (where k_{H^+} is the rate constant for proton transfer onto various substituted anilines, as defined in eq 6 and 7, at 25 °C in CD_3CN) vs. $-pK_{eq}$ for the following hydrides: $CpW(CO)_3H$ (●), $HMn(CO)_5$ (▲), $H_2Fe(CO)_4$ (□), and $HCo(CO)_4$ (○). The values of k_{H^+} and pK_{eq} are taken from Table IV. The lines are the best least-squares fit to the data for each hydride.

For the same reasons we chose aniline as our standard base for the kinetic acidity series, we have used a series of para-substituted anilines to construct our Brønsted plots of log k_{H^+} vs. log K_{eq}, where K_{eq} is the equilibrium constant for the deprotonation equilibrium (eq 7). Calculation of K_{eq}, however, requires knowledge of the

$$H\text{-}M + B \underset{k_b}{\overset{k_{H^+}}{\rightleftharpoons}} M^- + BH^+ \ (K_{eq}) \qquad (7)$$

thermodynamic basicities in CH_3CN of these substituted anilines. We therefore determined pK_a values in CH_3CN for perchloric acid derivatives of the various substituted anilines. The results are shown in Table III.

The ^1H NMR line broadening techniques have been used to determine rate constants discussed above for proton transfer to these substituted anilines from $HMn(CO)_5$, $H_2Fe(CO)_4$, $HCo(CO)_4$, and $CpW(CO)_3H$. In the case of strongly acidic hydrides such as $HCo(CO)_4$ and $H_2Fe(CO)_4$, the actual concentration of aniline has been calculated from the concentration of aniline initially added, the known[12,16] pK_a of anilinium ion, and the known[1c] pK_a of $HCo(CO)_4$ or $H_2Fe(CO)_4$. The resulting values of k_{H^+}, extrapolated to 25 °C, are given in Table IV. Figure 1 shows plots of log k_{H^+} vs. $-pK_{eq}$ (= log K_{eq}) for each hydride. The values of $-pK_{eq}$ have been calculated according to eq 8, where

$$-pK_{eq} = pK_a(BH^+) - pK_a(MH) \qquad (8)$$

$pK_a(MH)$ is the hydride pK_a from the set of values we have recently reported[1c] and where $pK_a(BH^+)$ is the pK_a of the perchloric acid derivative of the substituted aniline (Table III). For $HMn(CO)_5$ the resulting value of the Brønsted slope, α, is 0.54, for $HW(CO)_3Cp$ α is 0.65, for $H_2Fe(CO)_4$ α is 0.55, and for $HCo(CO)_4$ α is 0.48.

The same ^1H NMR line broadening techniques have also been used to measure the rate constants for proton transfer onto aniline from most of the common mononuclear hydrides. The results, shown in Table V, have been measured at, or more often extrapolated down to, 25 °C. Comparison of k_{H^+} from $H_2Fe(CO)_4$ to aniline (Table V) with k_{self} from $H_2Fe(CO)_4$ onto $HFe(CO)_4^-$ (Table II) shows that transfer to aniline is more than 10 times

Table IV. Proton-Transfer Rates onto Para-Substituted Anilines in Acetonitrile at 25 °C

MH	base	pK_{eq}[a,b]	k_{H^+}, M^{-1} s^{-1}	$\Delta H^{\ddagger}$,[b] kcal mol^{-1}	$\Delta S^{\ddagger}$,[b] eu
$Cp(CO)_3WH$	*p*-cyanoaniline	8.5 (1)	3.0 (2) × 10^0	7.0 (3)	−31.2 (8)
$Cp(CO)_3WH$	ethyl *p*-aminobenzoate	7.9 (1)	8.0 (5) × 10^0	7.3 (4)	−30.0 (10)
$Cp(CO)_3WH$	*p*-iodoaniline	6.6 (1)	5.1 (1) × 10^1	6.2 (2)	−29.9 (5)
$Cp(CO)_3WH$	aniline	5.5 (1)	2.5 (1) × 10^2	6.3 (4)	−26.2 (10)
$Cp(CO)_3WH$	*p*-methylaniline	5.0 (1)	6.8 (7) × 10^2	5.1 (1)	−28.6 (4)
$Cp(CO)_3WH$	*p*-methoxyaniline	4.8 (1)	8.3 (2) × 10^2	4.9 (2)	−28.6 (7)
$(CO)_5MnH$	*p*-cyanoaniline	7.5 (1)	4.0 (1) × 10^0	6.7 (3)	−33.2 (9)
$(CO)_5MnH$	ethyl *p*-aminobenzoate	6.9 (1)	1.5 (5) × 10^1	6.9 (4)	−29.7 (13)
$(CO)_5MnH$	*p*-bromoaniline	5.5 (1)	6.5 (6) × 10^1	6.4 (3)	−28.6 (5)
$(CO)_5MnH$	aniline	4.5 (1)	2.1 (1) × 10^2	4.9 (3)	−31.3 (9)
$(CO)_5MnH$	*p*-methylaniline	4.0 (1)	4.2 (4) × 10^2	4.8 (2)	−27.2 (9)
$(CO)_4FeH_2$	*p*-cyanoaniline	3.8 (1)	7.6 (8) × 10^2	4.9 (2)	−29.0 (10)
$(CO)_4FeH_2$	2,4-dichloroaniline	3.4 (1)	1.1 (1) × 10^3	4.5 (1)	−29.3 (4)
$(CO)_4FeH_2$	ethyl *p*-aminobenzoate	3.2 (1)	1.9 (1) × 10^3	3.5 (2)	−31.7 (7)
$(CO)_4FeH_2$	*p*-iodoaniline	1.9 (1)	7.4 (2) × 10^3	3.5 (6)	−28.9 (2)
$(CO)_4FeH_2$	aniline	0.8 (1)	5.4 (4) × 10^4	4.0 (2)	−23.7 (10)
$(CO)_4CoH$	aniline	−2.3 (2)	1.7 (5) × 10^6	2.9 (2)	−20.2 (6)
$(CO)_4CoH$	*p*-iodoaniline	−1.2 (2)	2.4 (1) × 10^5	2.9 (3)	−27.5 (5)
$(CO)_4CoH$	*p*-(trifluoromethyl)aniline	−0.3 (2)	9.5 (6) × 10^4	4.3 (2)	−21.3 (7)
$(CO)_4CoH$	ethyl *p*-aminobenzoate	0.1 (2)	7.7 (9) × 10^4	4.4 (2)	−21.4 (12)
$(CO)_4CoH$	2,4-dichloroaniline	0.3 (2)	5.2 (3) × 10^4	3.9 (2)	−26.9 (7)
$(CO)_4CoH$	*p*-cyanoaniline	0.7 (2)	4.1 (4) × 10^4	3.6 (3)	−25.4 (9)

[a] $pK_a(MH) - pK_a(baseH^+)$ from ref 1c, ref 12, and Table III. [b] Numbers in parentheses are the estimated standard deviations in the least significant figure.

Table V. Proton-Transfer Rates onto Aniline in Acetonitrile at 25 °C

MH	base	pK_{eq}[a,b]	k_{H^+},[b] M^{-1} s^{-1}	$\Delta H^{\ddagger}$,[b] kcal mol^{-1}	$\Delta S^{\ddagger}$,[b] eu
$(CO)_4CoH$	aniline	−2.3 (2)	1.7 (5) × 10^6	2.9 (2)	−20.2 (6)
$(CO)_4FeH_2$	aniline	0.8 (1)	5.4 (4) × 10^4	4.0 (2)	−23.7 (10)
$Cp(CO)_3CrH$	aniline	2.7 (1)	1.7 (1) × 10^4	3.8 (2)	−26.4 (6)
$Cp(CO)_3MoH$	aniline	3.3 (1)	3.9 (3) × 10^3	4.4 (1)	−27.4 (5)
$Cp(CO)_3WH$	aniline	5.5 (1)	2.5 (1) × 10^2	6.3 (4)	−26.2 (10)
$(CO)_5MnH$	aniline	4.5 (1)	2.1 (1) × 10^2	4.9 (3)	−31.3 (9)
$C_5Me_5(CO)_3MoH$	aniline	6.5 (1)	4.9 (2) × 10^1	7.1 (2)	−26.5 (8)
$(CO)_4RuH_2$	aniline	8.1 (1)	8.0 (15) × 10^0	8.5 (5)	−25.9 (12)
$Cp(CO)_2FeH$	aniline	8.8 (1)	4.0 (3) × 10^{-1}	9.0 (4)	−30.2 (11)
$(CO)_4OsH_2$	aniline	10.2 (1)	1.0 (4) × 10^{-2} [c]	14.7 (7)	−18.3 (20)
$(CO)_4OsH_2$	aniline-d_2	...	6.1 (2) × 10^{-3} [d]	...	...
$(CO)_5ReH$	aniline	10.5 (3)	1.4 (9) × 10^{-2} [c]	12.9 (11)	−23.0 (19)
$(CO)_5ReH$	aniline-d_2	...	1.0 (3) × 10^{-3} [d]	...	...
$Cp(PMe_3)(CO)_2WH$	aniline	16.0 (2)	$<10^{-3}$	...	...

[a] $pK_a(MH) - pK_a(baseH^+)$ from ref 1c and ref 12. [b] Numbers in parentheses are the estimated standard deviations in the least significant figure. [c] Estimated from the increase in line width of MH in the presence of aniline, over the line width of a solution adjusted to the same viscosity by the addition of diphenyl ether. [d] Measured by isotope exchange (eq 13).

faster than transfer to $HFe(CO)_4^-$, despite the fact that the latter is a stronger base (the pK_a of $H_2Fe(CO)_4$[1c] is 11.4, whereas that of $PhNH_3^+$ is 10.6[12,16]). These results further illustrate the generalization quoted[1a,b] in the introduction: given the same thermodynamic driving force, a proton transfer to a metal base faces a higher kinetic barrier than a proton transfer to a nitrogen base.

The measurement of extremely slow rates of proton transfer by line width methods proved difficult, particularly if there was a significant line width in the absence of exchange. For $HMn(CO)_5$, $HRe(CO)_5$, and $HCo(CO)_4$ such a line width[18] arises from residual coupling[19] to metal nuclei with $I = {}^5/_2$ (Mn, Re) or $I = {}^7/_2$ (Co). Its magnitude depends upon the efficiency of quadrupolar relaxation, and consequent decoupling, of these metal nuclei and thus upon the molecular correlation time τ_c of these complexes. If the macroscopic shear viscosity η is constant, τ_c, the rate of quadrupolar relaxation of the metal nucleus, and the ^1H NMR line width from residual coupling to the metal nucleus should also remain constant.[19,20]

With $HMn(CO)_5$ and $HCo(CO)_4$ the proton-transfer rates proved sufficiently fast that the concentrations of aniline required to produce a significant increase in line width were small enough to permit neglect of their effect on the viscosity of the solution; it was therefore possible to assume that the line width due to residual ^{55}Mn or ^{59}Co coupling was the same in pure CD_3CN as in the presence of aniline in the same solvent at the same temperature. With $HRe(CO)_5$, however, the concentrations of aniline required to produce observable broadening of the ^1H resonance were obviously large enough to affect the viscosity and therefore to affect the residual coupling to ^{185}Re and ^{187}Re; we therefore subtracted the line width of $HRe(CO)_5$ in a solution of the same macroscopic viscosity but without any kinetically active base. (We measured the macroscopic viscosities of the concentrated solutions of aniline in acetonitrile used for the rate measurements and then duplicated them by adding appropriate quantities of diphenyl ether to acetonitrile at the same temperatures.) Even at high temperatures and high aniline concentrations, however, the line width increase due to proton transfer was small compared to the residual line width from Re coupling, and the resulting $HRe(CO)_5/PhNH_2$ rate constants were therefore not very accurate.

More accurate measurements of the $HRe(CO)_5/PhNH_2$ rate constant, and of the almost equally slow $H_2Os(CO)_4/PhNH_2$ rate

(18) Line widths in CD_3CN in the absence of exchange at temperatures typical of the k_{H^+} experiments were as follows: $HMn(CO)_5$, 1.4 Hz, 7 °C; $HRe(CO)_5$, 1.4 Hz, 67 °C; $HCo(CO)_4$, 27 Hz, −43 °C.

(19) (a) Whitesides, G. M.; Mitchell, H. L. *J. Am. Chem. Soc.* **1969**, *91*, 2245. (b) Akitt, J. W. *N.M.R. and Chemistry*; Chapman and Hall, Ltd.: London, 1973; pp 85–8. (c) Harris, R. K. *Nuclear Magnetic Resonance Spectroscopy*; Pitman Books: London, 1983; pp 133–40.

(20) Farrar, T. C.; Becker, E. D. *Pulse and Fourier Transform NMR*; Academic: New York, 1971; pp 58–9.

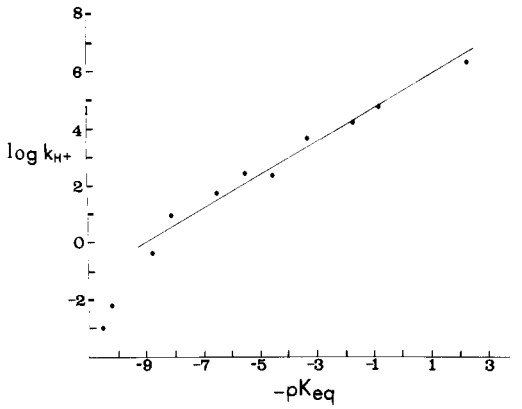

Figure 2. Plot of log k_{H^+} (where k_{H^+} is the rate constant for proton transfer onto aniline, as defined in eq 6 and 7, at 25 °C in CD_3CN) vs. $-pK_{eq}$. The values of k_{H^+} and pK_{eq} are taken from Table V. The line is the best least-squares fit to the data for all hydrides except $HRe(CO)_5$ and $H_2Os(CO)_4$.

constant, were obtained by watching the approach to equilibrium of mixtures of these hydrides with $PhND_2$ (eq 9 and 10). If the rate constant k_{HD} for exchange between an H site on M and a D site on $PhND_2$ is defined as in eq 11, the ratio of k_{HD} to the reverse rate constant k_{DH} depends upon the magnitude of any equilibrium isotope effects present. (In eq 11 m is the number of equivalent H sites on the metal, one for $HRe(CO)_5$ and two for $H_2Os(CO)_4$.) If such isotope effects were absent (i.e., if k_{HD} were equal to k_{DH}), such systems would approach equilibrium by a first-order rate constant $k_{obsd}(equil)$, related to k_{HD} by the generalized McKay equation (eq 12).[21,22]

$$HRe(CO)_5 + PhND_2 \rightleftarrows DRe(CO)_5 + PhNHD \quad (9)$$

$$H_2Os(CO)_4 + PhND_2 \rightleftarrows HDOs(CO)_4 + PhNHD \rightleftarrows D_2Os(CO)_4 + PhNH_2 \quad (10)$$

$$MH_{m-x}D_x + PhNH_yD_{2-y} \underset{k_{DH}}{\overset{k_{HD}}{\rightleftharpoons}} MH_{m-x-1}D_{x+1} + PhNH_{y+1}D_{2-y-1} \quad (11)$$

$$k_{obsd}(equil) = k_{HD}\left[\frac{m[MH_m]_{t=0} + 2[PhND_2]_{t=0}}{2m}\right] \quad (12)$$

In the case of metal–nitrogen proton transfer, however, a substantial equilibrium isotope effect is expected (k_{HD}/k_{DH} can be estimated at 0.40[23,24]). Thus these exchange reactions will not in general approach isotopic equilibrium by first-order processes. However, if $[PhND_2]$ is sufficiently large ($\gg [MH_m]$) and if deuterium incorporation into $PhND_2$ is sufficiently complete, k_{HD} can be obtained by watching the disappearance, rate constant k^H_{obsd} of the MH_m ^1H NMR signal. Multiplying k^H_{obsd}, the proton replacement rate constant, by m gives the first-order rate constant for replacement of any single H in a molecule of MH_m by D; division by $[PhND_2]$ gives the second-order rate constant k_{HD} as defined in eq 11. As all deprotonations of MH_m result in replacement by D of the H removed,[25] k_{HD} equals k_{H^+} as defined in eq 6. The values of k_{H^+} from eq 13 for $H_2Os(CO)_4/PhND_2$

$$k_{H^+} = mk_{obsd}(H)/[PhND_2] \quad (13)$$

and $HRe(CO)_5/PhND_2$ are given in Table V along with the k_{H^+} values obtained for $H_2Os(CO)_4/PhNH_2$ and $HRe(CO)_5/PhNH_2$ by the line broadening methods discussed above, although the precision and accuracy of the former set of k_{H^+} values are much higher. (It seems unlikely that k_{H^+} for deprotonation by $PhND_2$ differs appreciably from k_{H^+} for deprotonation by $PhNH_2$.)

If the k_{H^+} data in Table V are plotted vs. $-pK_{eq}$ for their equilibrium deprotonation by aniline (Figure 2), a reasonable linear correlation is obtained,[26] despite the fact the geometry of the transition state is obviously different for the different hydrides. These results suggest that there is at least a rough correlation between rate and thermodynamic driving force for all proton transfer reactions of these hydrides and that the relative rates in Table V can be used as a diagnostic kinetic acidity series.

We have tested this approach on the reaction forming methane and a heterobimetallic complex from Cp_2ZrMe_2 and $HM(CO)_3Cp$ (M = Cr, Mo, W) (reaction 14). For M = Mo the product has

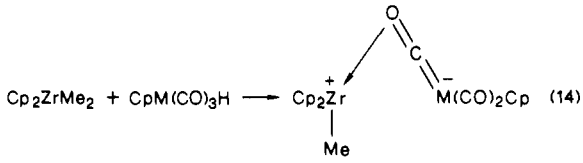

been shown crystallographically to have the carbonyl-*O,C* bridged structure illustrated, and considerable spectroscopic evidence suggests that the M = Cr and M = W products are isostructural.[9] This structure suggests that these compounds can be viewed as ion pairs. Conductivity measurements show slight dissociation in CH_3CN for M = W and Mo and substantial dissociation in CH_3CN for M = Cr.

Exchange of $M(CO)_3Cp^-$ Units between $CpM(CO)_3H$ and $Cp_2ZrMe(\mu\text{-}OC)M(CO)_2Cp$. ^1H NMR studies of reaction 15

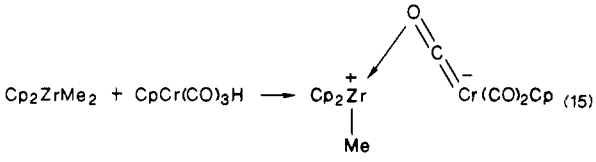

showed evidence of some exchange process involving $CpCr(CO)_3H$ and $Cp_2ZrMe(\mu\text{-}OC)Cr(CO)_2Cp$. During a kinetics run at −6 °C in CD_3CN (involving equimolar amounts of Cp_2ZrMe_2 and $CpCr(CO)_3H$), a single coalesced NMR signal due to the Cr cyclopentadienyl rings of $Cp_2ZrMe(\mu\text{-}OC)Cr(CO)_3Cp$ and of $CpCr(CO)_3H$ was observed. During the intermediate portion of the kinetics run, the merged Cr Cp peak showed a substantial line width (≈25 Hz) not present in the initial ($CpCr(CO)_3H$) and final ($Cp_2ZrMe(\mu\text{-}OC)Cr(CO)_2Cp$) peaks. As the reaction progressed, the center of the peak shifted from δ 4.95 to 4.45, i.e., from the chemical shift of the chromium cyclopentadienyl ring of pure $CpCr(CO)_3H$ to that of pure $Cp_2ZrMe(\mu\text{-}OC)Cr(CO)_2Cp$. At −20 °C and below, the Cr Cp peaks of hydride and product appeared as two separate resonances but did show broadening which decreased with decreasing temperature. No broadening of any other peaks was observed at any temperature.

(21) McKay, H. A. C. *J. Am. Chem. Soc.* **1943**, *65*, 702.
(22) Harris, G. M. *Trans. Faraday Soc.* **1951**, *47*, 716.
(23) For M–H + N–D ⇄ M–D + N–H, the equilibrium constant can be estimated by

$$K = \frac{\exp(+(hc/2kT)(\nu(M\text{–}H) - (\nu(M\text{–}D))}{\exp(-(hc/2kT)(\nu(N\text{–}H) - (\nu(N\text{–}D))}$$

if the general expression[24] is modified to consider only stretching vibrations. Taking ν(M–H) as 1845 cm^{-1}, ν(M–D) as 1322 cm^{-1} (as in the calculation of kinetic isotope effects at the beginning of the Results), ν(N–H) as 3355 cm^{-1}, and ν(N–D) as 2425 cm^{-1} yields 0.37 for the equilibrium constant. An equilibrium isotope effect of about one-half has typically been observed for a closely related system, M–H + C–D ⇄ M–D + C–H (see: Bullock, R. M.; Headford, C. E. L.; Kegley, S. E.; Norton, J. R. *J. Am. Chem. Soc.* **1985**, *107*, 727 and references therein).
(24) Wiberg, K. W. *Physical Organic Chemistry*; Wiley: New York, 1964; p 275.
(25) For reasons explained earlier,[17] $PhNHD_2^+$ will react much more rapidly with $PhND_2$ than with the metal anion formed by deprotonation. Calculations based on the concentrations present in an actual $H_2Os(CO)_4/PhND_2$ run show that proton exchange by $PhNHD_2^+$ will be about 10^5 times as fast as reprotonation.
(26) Most of the data plotted in Figure 2 show a monotonic increase in k_{H^+} with increased thermodynamic driving force, but k_{H^+} for $HMn(CO)_5$ is slightly slower than that for $HW(CO)_3Cp$. We have checked the relative pK_a values for $HW(CO)_3Cp$ and $HMn(CO)_5$ by measuring the equilibium constant for $HMn(CO)_5 + [W(CO)_3Cp]^- \rightleftarrows [Mn(CO)_5]^- + HW(CO)_3Cp$; the measured pK_{eq} is 1.1, in excellent agreement with that (1.0) calculated from our pK_a values.

Table VI. Observed Pseudo-First-Order Rate Constants for Reaction 14 (M = W) When Either Reagent Is Present in Excess[a]

excess reagent	$10^5 k_{obsd}$,[b] s^{-1}	concn of excess reagent (M)
Cp_2ZrMe_2	4.3 (1)[c]	1.38
Cp_2ZrMe_2	3.25 (8)[c]	1.15
Cp_2ZrMe_2	7.6 (2)[c]	2.61
Cp_2ZrMe_2	5.7 (2)[c]	2.03
Cp_2ZrMe_2	1.2 (4)[c]	0.55
$CpW(CO)_3H$	2.22 (5)[d]	0.89
$CpW(CO)_3H$	4.28 (7)[d]	1.61
$CpW(CO)_3H$	6.75 (8)[d]	2.34

[a] In THF at 50 °C. [b] Numbers in parentheses are the estimated standard deviations in the least significant figure. [c] Pseudo-first-order rate constant for disappearance of $CpW(CO)_3H$. [d] Pseudo-first-order rate constant for disappearance of Cp_2ZrMe_2.

These results suggested an exchange of $CpCr(CO)_3^-$ units between product and $CpCr(CO)_3H$. Such exchange was confirmed by ^1H NMR study of a solution of $Cp_2ZrCH_3(\mu\text{-}OC)Cr(CO)_2Cp$ before and after addition of $CpCr(CO)_3H$. The initial sharp resonance of the Cr Cp of $Cp_2ZrCH_3(\mu\text{-}OC)Cr(CO)_2Cp$ broadened after the $CpCr(CO)_3H$ was added. The variable-temperature spectra of the mixture replicated those described in the previous paragraph: at −20 °C and below, the Cr Cp resonances appeared as two distinct peaks, both substantially broadened; at −6 °C the two Cr Cp peaks had coalesced.

Broadening of Cr Cp peaks was also observed during kinetics measurements in THF, although the cyclopentadienyl peaks never coalesced in that solvent, even at 25 °C. No evidence for such an exchange process was seen with the Mo and W hydrides in any solvent. The comparatively rapid exchange between $CpCr(CO)_3H$ and $Cp_2ZrMe(\mu\text{-}OC)Cr(CO)_2Cp$ is not surprising in view of the greater dissociation of the latter in CH_3CN (as shown by the conductivity measurements above).

Kinetics of Reaction 14. Detailed examination of the kinetics of reaction 14 with M = W in THF has confirmed the presumption that the reaction obeys the rate law in eq 16. The data in Table

$$-\frac{d[Cp_2ZrMe_2]}{dt} = -\frac{d[CpM(CO)_3H]}{dt} = k_{16}[Cp_2ZrMe_2][CpM(CO)_3H] \quad (16)$$

VI show that the reaction obeys pseudo-first-order kinetics when either reactant is present in excess and that the pseudo-first-order rate constant is linear with respect to the excess reagent in both cases. The second-order rate constant k_{16} obtained from the data with Cp_2ZrMe_2 in excess (3.0 (1) × 10^{-5} M^{-1} s^{-1}) agrees with the second-order rate constant obtained from the data with $CpW(CO)_3H$ in excess. The assumption that the same rate law prevails in CH_3CN and for M = Cr and M = Mo has been supported by the observation of pseudo-first-order kinetics for the disappearance of $CpM(CO)_3H$ (M = Cr, Mo, W) in the presence of excess $CpZrMe_2$ and in a few cases by the observation of second-order kinetics with equal or near-equal initial reagent concentrations.

The observed second-order rate constants k_{16}, in CH_3CN and THF at various temperatures, are given in Table VII. As the instability of $CpMo(CO)_3H$ in CH_3CN near room temperature[1a] makes it impossible to measure the rate of the Cp_2ZrMe_2/$CpMo(CO)_3H$ reaction in that solvent above −6 °C, the other second-order rate constants have been extrapolated to that temperature for comparison; the resulting −6 °C values of k_{16} are given in Table VIII, as are values for k_{16} in THF extrapolated to 25 °C and the activation parameters in both solvents. For each metal the −6 °C k_{16} value in acetonitrile (ϵ = 37) is about 2 orders of magnitude greater than the −6 °C k_{16} value in THF (ϵ = 7.6).

The relative rates (W:Mo:Cr) are 1:18:81 in THF at 25 °C; they are 1:20:200 in CD_3CN at −6 °C. These relative rates agree remarkably well with those (1:16:68) from the proton-transfer rates in Table V (onto aniline from the same hydrides).

Discussion

Rate constants k_b for proton transfer from BH^+ to M^-, the back-reaction of eq 7, can be calculated for each case in Tables IV and V. The maximum calculated k_b values, about 10^9 M^{-1} s^{-1}, occur when pK_{eq} is largest, and the deprotonation equilibrium is most unfavorable (for example, $CpW(CO)_3H/p\text{-}NCC_6H_4NH_2$ and $H_2Ru(CO)_4/PhNH_2$). These maximum values closely approach the rate constants expected[27,28] for diffusion-controlled reactions in acetonitrile at 25 °C.

Table VII. Second-Order Rate Constants k_{16} for Reactions 14 at Various Temperatures

solv	[CpM-$(CO)_3H$]	M	[Cp_2Zr-Me_2]	k_{16},[a] M^{-1} s^{-1}	T,[a] °C
THF	0.122	W	1.25	9.67 (5) × 10^{-5}	65.0 (1)
THF	0.275	W	2.93	1.51 (4) × 10^{-5}	40.0 (2)
THF	0.283	W	2.85	0.93 (2) × 10^{-5}	31.2 (2)
THF	0.0755	Mo	0.790	4.8 (1) × 10^{-4}	50.0 (1)
THF	0.0261	Mo	0.311	2.3 (2) × 10^{-4}	40.0 (1)
THF	0.0770	Mo	0.971	1.58 (5) × 10^{-4}	31.2 (2)
THF	0.0844	Mo	0.989	0.63 (1) × 10^{-4}	20.3 (2)
THF	0.0900	Cr	1.20	4.4 (2) × 10^{-4}	25.0 (2)
THF	0.125	Cr	1.25	1.5 (7) × 10^{-4}	10.7 (2)
THF	0.174	Cr	2.25	0.86 (3) × 10^{-4}	0.7 (2)
THF	0.150	Cr	2.30	3.43 (6) × 10^{-5}	−10.3 (1)
CD_3CN	0.0234	W	0.315	7.3 (3) × 10^{-3}	46.5 (1)
CD_3CN	0.0504	W	0.504	2.7 (1) × 10^{-3}	35.1 (2)
CD_3CN	0.0360	W	0.363	9.8 (4) × 10^{-4}	23.0 (2)
CD_3CN	0.0521	W	0.529	4.3 (3) × 10^{-4}	15.3
CD_3CN	0.0260	Mo	0.268	9.0 (3) × 10^{-4}	−6.0 (1)
CD_3CN	0.0760	Cr	0.076	9.1 (3) × 10^{-3}	−6.5 (1)
CD_3CN	0.0149	Cr	0.157	2.37 (7) × 10^{-3}	−20.0 (1)
CD_3CN	0.0143	Cr	0.165	1.3 (8) × 10^{-3}	−26.5 (1)
CD_3CN	0.0250	Cr	0.262	7.4 (3) × 10^{-4}	−34.0 (1)

[a] Numbers in parenthese are the estimated standard deviations in the least significant figures.

The Brønsted plots in Figure 1 (for $CpW(CO)_3H$, $H_2Fe(CO)_4$, $HMn(CO)_5$, and $HCo(CO)_4$ vs. various para-substituted anilines) are linear over a significant range of change in their thermodynamic driving forces (2–4 pK_a units). From the standpoint of Marcus theory such linearity implies a large intrinsic barrier, $\Delta G_0^{\ddagger}$, because the variation in α with $\Delta G°$ (and therefore with ΔpK_{eq}) should be given by eq 19 if $\Delta G^{\ddagger}$ is given by eq 17 and α is given by eq 18.[3-8] ($\Delta G_0^{\ddagger}$ is defined as the activation energy when $\Delta G°$

$$\Delta G^{\ddagger} = (1 + \Delta G°/4\Delta G_0^{\ddagger})^2 \Delta G_0^{\ddagger} \quad (17)$$

$$\alpha = \frac{\partial \Delta G^{\ddagger}}{\partial \Delta G°} = \frac{1 + \Delta G°/4\Delta G_0^{\ddagger}}{2} \quad (18)$$

$$\frac{d\alpha}{d\Delta G°} = \frac{1}{8\Delta G_0^{\ddagger}} \quad (19)$$

is zero, i.e., when the reaction is thermoneutral; $\Delta G^{\ddagger}$ is the activation energy for the proton transfer process with the thermodynamic driving force $\Delta G°$.) In view of the substantial barrier that apparently exists to the protonation and deprotonation of transition metals, one would expect $d\alpha/d\Delta G°$ to be extremely small, α therefore to remain constant over a large pK_{eq} range, and the Brønsted plot therefore to be linear, as observed, over that same range.[4]

In its simplest form,[3,4] Marcus theory also predicts that α should (as seen from eq 18) decrease toward 0.5 as the thermodynamic driving force $\Delta G°$ approaches zero (i.e., as the pK_a of the hydride decreases toward that of the anilinium cations). The decrease in α in the order $HW(CO)_3Cp > HMn(CO)_5 \approx H_2Fe(CO)_4 >$

(27) The bimolecular self-reaction of *tert*-butyl radicals in acetonitrile is largely diffusion-controlled and has a rate constant, $2k_t$, of 7.1 × 10^9 M^{-1} s^{-1} at 25 °C: Schuh, H.-H.; Fischer, H. *Helv. Chim. Acta* **1978**, *61*, 2130. (As $2k_t$ is the rate constant for pairwise disappearance of the radicals, the corresponding rate constant for the disappearance of each of two unlike species is half the value given, or k_t.) The bimolecular self-reaction of isopropylol radicals in acetonitrile is also largely diffusion-controlled and has a rate constant, $2k_t$, of 2.7 × 10^9 M^{-1} s^{-1} at 25 °C: Lehni, M.; Fischer, H. *Int. J. Chem. Kinet.* **1983**, *15*, 733. We thank Prof. J. Halpern for bringing these references to our attention.

(28) Strohbusch, Marshall, and Eyring[15b] have estimated the rate constant for a diffusion-controlled proton transfer in acetonitrile at 25 °C to be 5 × 10^{10} M^{-1} s^{-1} between ions the size of protonated methyl red and picrate ion.

Table VIII. Extrapolated Second-Order Rate Constants k_{16} for Reaction 14

solv	M in $CpM(CO)_3H$	k_{16}(−6 °C),[a] M^{-1} s^{-1}	k_{16}(25 °C),[a] M^{-1} s^{-1}	$\Delta H^{\ddagger}$,[a] kcal/mol	$\Delta S^{\ddagger}$,[a] eu
THF	W	3.1 (8) × 10^{-7}	5.2 (5) × 10^{-6}	13.6 (9)	−36 (3)
THF	Mo	8 (1) × 10^{-6}	9.2 (6) × 10^{-5}	11.8 (9)	−37 (3)
THF	Cr	4.9 (3) × 10^{-5}	4.2 (3) × 10^{-4}	10.4 (5)	−39 (2)
CD_3CN	W	4.5 (4) × 10^{-5}	1.1 (5) × 10^{-3}	15.7 (3)	−19 (1)
CD_3CN	Mo	9.0 (4) × 10^{-4} [b]	...	...	...
CD_3CN	Cr	8.7 (9) × 10^{-3}	9 (1) × 10^{-2}	11.6 (8)	−26 (3)

[a] Numbers in parentheses are the estimated standard deviations in the least significant figure. [b] Measured directly at −6 °C because of the instability of $CpMo(CO)_3H$ in CD_3CN at higher temperatures.

$HCo(CO)_4$ is approximately as predicted; pK_{eq} at the midpoint of the Brønsted plot is about 6.5 for $HW(CO)_3Cp$, about 5.5 for $HMn(CO)_5$, about 2.5 for $H_2Fe(CO)_4$, and about zero for $HCo(CO)_4$. However, the low symmetry of M–H/N–H proton transfers (the M–H force constants are certainly quite different from the N–H ones, as reflected in the equilibrium isotope effects calculated in the Results[23]) means that departures from this simple prediction are to be expected.[4]

Extrapolation (or, in the case of $HCo(CO)_4$, interpolation) of the Brønsted plots in Figure 1 to thermoneutrality (pK_{eq} and $\Delta G°$ equal to zero) gives the intrinsic barriers to proton transfer from these hydrides to our substituted anilines. For $CpW(CO)_3H$ $\Delta G_0^{\ddagger}$ is 9.3 (2) kcal/mol, for $HMn(CO)_5$ it is 10.9 (3) kcal/mol, for $H_2Fe(CO)_4$ it is 10.7 (2) kcal/mol, and for $HCo(CO)_4$ it is 10.7 (5) kcal/mol. A physically reasonable interpretation of these values is that $\Delta G_0^{\ddagger}$ is smaller for seven-coordinate hydrides like $CpW(CO)_3H$ than for six- and five-coordinate ones like $HMn(CO)_5$, $H_2Fe(CO)_4$, and $HCo(CO)_4$. Marcus theory predicts that $\Delta G_0^{\ddagger}$ for W→N should be the average of $\Delta G_0^{\ddagger}$ for W→W and $\Delta G_0^{\ddagger}$ for N→N,[3-8] and 9.3 kcal/mol ($\Delta G_0^{\ddagger}$ for W→N) is about what we would expect for the average of 13.6 kcal/mol (the W→W intrinsic barrier calculated from k_{self} for $CpW(CO)_3H/CpW(CO)_3^-$) with the intrinsic barrier for N→N self-exchange (which is undoubtedly much smaller). In contrast, 10.7 kcal/mol ($\Delta G_0^{\ddagger}$ for Fe→N) is higher than we would expect for the average of 12.5 kcal/mol (the Fe→Fe intrinsic barrier calculated from the data in Table II) and the intrinsic barrier for N→N self-exchange.

Of course Figure 2, which displays the relation between $\Delta G^{\ddagger}$ and $\Delta G°$ for the rates of proton transfer onto aniline from all the transition-metal hydrides employed in this study, shows more departures from linearity than does Figure 1; changes in the metal to which the proton is bound before transfer should change the transition-state geometry in ways not directly attributable to changes in $\Delta G°$. The points in Figure 2 nevertheless form a reasonable straight line,[29] with a slope (0.58) similar to that of the Brønsted plots for single hydrides in Figure 1. If similar slopes are observed for proton transfers from the same hydrides to bases other than aniline, the relative reactivities of these hydrides toward any given base will be the same as in Figure 2. We do not expect that α will be constant in *all* proton transfer reactions of *all* metal hydrides; we do suggest that it may be sufficiently so to enable us to recognize the operation of proton-transfer mechanisms.

As noted in the Results, the relative reactivities of the various $HM(CO)_3Cp$ (M = Cr, Mo, W) in reaction 14 agree well with their relative proton-transfer rates toward aniline in the diagnostic kinetic acidity series (Table V). We therefore conclude that reaction 14 occurs by a proton-transfer mechanism. While the $\Delta S^{\ddagger}$ values for reaction 14 in CH_3CN (see Table VIII) fall in the same general range (about −20 to −28 eu) characteristic of proton-transfer reactions of all types in that solvent (note the values for anionic/neutral self-exchange reactions in Tables I and II, the values for hydride/aniline transfers in Table V, and the literature[30] values for deprotonations of carbon acids), the substantially more negative values of $\Delta S^{\ddagger}$ found for reaction 14 in THF (a solvent of lower dielectric constant) do offer supporting evidence that the mechanism of that reaction involves a highly charged transition state. Although the actual site of protonation is unclear (it cannot be the Zr(IV), as formally d° metals are highly resistant to nucleophilic attack,[31] but may in principle involve either front- or back-side attack on the methyl ligand), the transition state drawn in eq 20 seems the most reasonable possibility.

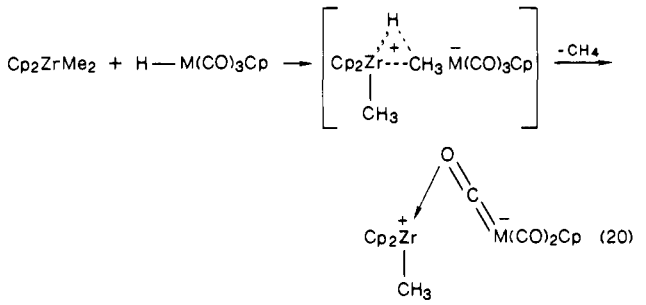

(20)

It is not surprising that Cp_2ZrMe_2, an organometallic complex of highly electropositive Zr, reacts with the acidic $HM(CO)_3Cp$ complexes by a proton transfer mechanism; the Zr–C bond in Cp_2ZrMe_2 is very reactive toward many protic reagents, including water.[32] We do believe that the approach we have used to establish this will prove generally useful. For example, Jacobsen and Bergman have already used[33] the kinetic acidity data reported herein to rule out a proton-transfer mechanism for the reaction of $CpMo(CO)_3H$ with $Cp_2Co_2(CO)_2(\mu\text{-}CCH_2)$.

Experimental Section

General Data. ^1H NMR spectra and kinetic data were recorded on a JEOL FX-100 or an IBM WP-200-SY spectrometer. Temperatures (−43 to 25 °C) were checked with a methanol thermometer.[34] The uncertainty in temperature was ±1 °C between −45 and 100 °C.

All manipulations were performed in an inert atmosphere (N_2) with high vacuum line, Schlenk, or inert atmosphere box techniques. Toluene, hexane, diethyl ether, glyme, diglyme, tetraglyme, and THF used in standard preparations were distilled under N_2 from Na- or K/benzophenone. Benzene and benzene-d_6 were dried over P_4O_{10}, frozen, and degassed at least three times and transferred under vacuum. THF, used for NMR kinetics, was first distilled under N_2 from Na/benzophenone, then vacuum distilled from sodium, and then triply distilled in vacuo. Acetonitrile-d_3 was distilled under vacuum from P_4O_{10} after the minimum necessary drying time (15 min).

Aniline, *p*-(trifluoromethyl)aniline, and *p*-fluoroaniline were predried over, and then fractionally distilled from, barium oxide. 2,4-Dichloroaniline, *p*-iodoaniline, *p*-bromoaniline, ethyl *p*-aminobenzoate, *p*-cyanoaniline, *p*-toluidine, and *p*-anisidine were recrystallized from ethanol and dried in vacuo for 6 h at 40 °C. Aniline-*N*-d_2 (each site >98% deuter-

(29) Bell,[5] p 203, shows that the rate and equilibrium constants for the reaction of a variety of carbon acids (ketones, esters, and keto-esters) with a variety of bases all fall on or near the same smooth curve, which is approximately linear over substantial ranges of thermodynamic driving force. There is thus precedent for approximately linear relationships between $\Delta G^{\ddagger}$ and $\Delta G°$ in proton transfer reactions where there is significant variation in transition-state geometry.

(30) (a) Caldin, E. F.; Jarczewski, A.; Leffek, K. T. *Trans. Faraday Soc.* **1971**, *67*, 110. (b) Caldin, E. F.; Mateo, S. *J. Chem. Soc., Faraday Trans. 1* **1975**, *71*, 1876. (c) Caldin, E. F.; Wilson, C. J. *Symp. Faraday Soc.* **1975**, *10*, 121.

(31) Collman, J. P.; Hegedus, L. S.; Norton, J. R.; Finke, R. F. *Organotransition Metal Chemistry*; University Science Books: Mill Valley, CA, 1987; Chapter 8.

(32) Wailes, P. C.; Coutts, R. S. P.; Weigold, H. *Organometallic Chemistry of Titanium, Zirconium, and Hafnium*; Academic: New York, 1974, p 151.

(33) See footnote 22 in: Jacobsen, E. N.; Bergman, R. G. *J. Am. Chem. Soc.* **1985**, *107*, 2023.

(34) Van Geet, A. L. *Anal. Chem.* **1970**, *42*, 679.

iated) was prepared by extracting 2 mL of aniline with eight 1-mL portions of D_2O (99% d) and fractionally distilling the aniline from CaO; percent deuterium incorporation was determined by ^1H NMR integration. (All glassware used for $PhND_2$ preparation was treated with D_2O and heated under dynamic vacuum.) Trifluoroacetic acid was distilled from a small amount of P_4O_{10} prior to use. $Co_2(CO)_8$ was sublimed at 25 °C under vacuum prior to use.

Picric acid was purified by the method of Kolthoff and Chantooni.[16] Tetraethylammonium perchlorate was dried in vacuo at 70 °C. Tetra-*n*-butylammonium picrate was prepared by titrating a 400-mL aqueous solution of picric acid (2 g) to slightly beyond the equivalence point with a 55% aqueous solution of tetra-*n*-butylammonium hydroxide. The water was then distilled off, and the ammonium salt was dissolved in benzene and dried with 3-Å molecular sieves. The volume was reduced, and the ammonium salt was allowed to crystallize at room temperature. The crystals were filtered and recrystallized in benzene and then dried in vacuo at 70 °C for 12 h. $HClO_4$ (70%) was standardized and was determined to be 70.9% by titration with 1.00 M KOH to a phenolphthalein end point.

The following compounds were prepared by methods cited in our previous papers[1] on thermodynamic acidities: $Na[CpM(CO)_3]$, $K[CpM(CO)_3]$, $CpM(CO)_3H$ (M = Cr, Mo, and W), $HCo(CO)_4$, $H_2Fe(CO)_4$, $Na_2Fe(CO)_4$, $K_2Fe(CO)_4$, $[PPN][HFe(CO)_4]$, $H_2Ru(CO)_4$, $H_2Os(CO)_4$, $HM(CO)_5$ (M = Mn, Re), and $Cp^*Mo(CO)_3H$ ($Cp^* = \eta^5$-C_5Me_5). Cp_2ZrMe_2 was prepared by the method of Wailes, Weigold, and Bell.[35] $CpM(CO)_3D$ (M = Cr, Mo, W) was prepared by deuteriation of a THF solution of $K[CpM(CO)_3]$ with 85% D_3PO_4 in D_2O (99% *d*) followed by removal of THF by vacuum distillation and sublimation onto a water-cooled sublimation probe. The Cr–D stretching frequency, not previously published, proved to be 1260 cm^{-1}.

Determination of the pK_a in Acetonitrile of the Protonated Form of Substituted Anilines. These values were determined by the potentiometric method of Coetzee and Padmanabhan,[36] using the cell design of Kolthoff and Thomas.[37] The cell contained three compartments: a reference compartment, a salt bridge, and a sample compartment. The reference electrode was comprised of a silver-plated platinum wire which made electrical contact with a pool of mercury. The reference compartment was filled with 0.10 M silver nitrate in acetonitrile. The salt bridge compartment was filled with 0.1 M Et_4NClO_4. The salt bridge and the sample compartment were separated by a fine porosity glass sinter. A platinum spiral electrode was placed in the sample compartment through a polyethylene plug used to seal the compartment from the atmosphere. Electrical connection between the two half-cells was made by inserting the side arm of the reference half-cell into the salt bridge solution through a polyethylene plug.

Response of the electrode was tested by observing the potential readings of acetonitrile solutions of perchloric acid and was found to be reproducible. The electrode was then calibrated with buffer solutions of picric acid and tetra-*n*-butylammonium picrate. Taking the pK_a of picric acid as 11.0,[38] the potential of solutions with known hydrogen ion activities (pa_{H^+} ranging from 9.6 to 11.8) was measured and ranged between 90 and 260 mV. Acetonitrile solutions of the substituted anilines were then titrated with freshly prepared $HClO_4$ stock solutions. The potential readings were measured, and from them the hydrogen ion activity in these solutions was calculated. The pK_a values for the anilinium salts (shown in Table III) were calculated by using eq 21; the activity coefficient, f_{BH^+}, was estimated by the Debye–Hückel limiting law, eq 22.[38] The literature values[12,16,36] for anilinium perchlorate and *p*-toluidinium perchlorate were successfully reproduced.

$$K_A(BH^+) = (a_{H^+})[B]/(f_{BH^+})[BH^+] \quad (21)$$

$$-\log f_{BH^+} = 1.5(\text{ionic strength})^{1/2} \quad (22)$$

Proton-Transfer Rate Measurements by NMR Line Broadening. For determination of the H^+ transfer rates from each metal hydride, to aniline or substituted anilines, two CD_3CN solutions were sealed under vacuum in 5-mm NMR tubes; one contained the exchanging species (hydride and aniline) and an internal concentration standard, and the other, used to measure line width in the absence of exchange, consisted of a CD_3CN solution of the metal hydride only. As explained in our earlier papers on kinetic acidity,[1a,b] the first-order rate constants for proton transfer were calculated according to eq 23 from the excess line width (of the hydride resonance) due to exchange. Division of the first-order rate constants by the concentration of proton-accepting base (eq 24), and extrapolation to 25 °C, gave the second-order rate constants for proton transfer in Tables IV and V. The standard deviations of the extrapolated rate constants were calculated from the standard deviations and covariance of $\Delta H^\ddagger$ and $\Delta S^\ddagger$.[1a]

$$k(\text{first-order})^{MH,B} = \pi(\text{excess line width due to exchange}) \quad (23)$$

$$k_{H^+} = k(\text{first-order})^{MH,B}/[\text{base}] \quad (24)$$

In the case of measurements of self-exchange rate constants, solutions of the hydride and the anion were sealed together in one NMR tube, and a solution of one or the other alone was sealed in another tube in order to determine the line width in the absence of exchange. The first-order rate constant for the disappearance of M^- or MH was then determined (by the method of eq 23) from its excess line width in the presence of the other species, and k_{self} (Tables I and II) was calculated from that first-order rate constant by dividing it (in analogy with eq 24) by the concentration of the other species.

The kinetic deuterium isotope effects at 25 °C, given in Table I, were calculated by using eq 25. The H^+ transfer rate constant $k^H{}_{av}$ was the

$$\frac{k^H{}_{self}}{k^D{}_{self}} = \frac{k^H{}_{av}}{k(M^-,MD)(\text{corrected})} \quad (25)$$

average of the second-order rate constant $k(M^-,MH)$ (obtained by observing the line width of the ^1H NMR resonance of the cyclopentadienyl ligand of M^- in the presence of MH) and the second-order rate constant $k(MH,M^-)$ (obtained by observing the line width of the ^1H NMR resonance of the cyclopentadienyl ligand of MH in the presence of M^-).

Rate constants $k(M^-,MD)$ for M^-/MD transfer were corrected for MH impurities; the observed first-order rate constant for the disappearance of M^-, from the line width of the cyclopentadienyl resonance of M^-, included contributions from protonation of M^- by both MH and MD. True second-order rate constants for M^-/MD transfer, $k(M^-,MD)$(corrected), were calculated by using eq 26.

$$k(M^-,MD)(\text{corrected}) = \frac{k(M^-,MD)(\text{observed first-order}) - k^H{}_{av}[MH]}{[MD]} \quad (26)$$

In some cases, $HCo(CO)_4$ with all anilines and $H_2Fe(CO)_4$ with aniline itself, extensive deprotonation was observed, and equilibrium concentrations of all species ([MH], [aniline], [M^-], and [anilineH$^+$]) were estimated by using the integrated peak intensities in the NMR. These concentrations were in agreement with the equilibrium concentrations calculated from the thermodynamic acidities (pK_a) of the metal hydride and the protonated aniline.

The Measurement of the Viscosity of Acetonitrile Solutions of Aniline and Diphenyl Ether. All viscosity measurements were done with the use of an Ostwald viscosimeter by timing the passage of a known volume V of liquid through a capillary of known radius r and length L. The viscosimeter was calibrated with neat aniline, and viscosities were calculated according to eq 27. At 60 °C the macroscopic viscosity of a 2.3 M acetonitrile solution of diphenyl ether (η = 0.0048 cP) was approximately equal to that of a 3.2 M acetonitrile solution of aniline.

$$\eta = \pi r^4 Pt/8VL \quad (27)$$

Hydride Signals Broadened by Residual Coupling to Quadrupolar Nuclei. In the case of the $HRe(CO)_5/PhNH_2$ H^+ transfer experiment, the ^1H NMR line width of the $HRe(CO)_5$ contained contributions from the residual coupling to ^{185}Re and ^{187}Re as well as broadening due to the exchange process. By independently simulating the macroscopic viscosity of the aniline solution with a nonreactive, nonbasic substitute for aniline, the line width in the absence of exchange was determined and subtracted from the line width observed with aniline in order to determine the line broadening caused by proton transfer. Diphenyl ether has a viscosity that is similar to that of aniline; it was therefore used as an aniline substitute. The measured line width differences between the total line width and the line width contribution from residual coupling were small; as a result, the extrapolated rate constant (Table V) was very inaccurate.

$HRe(CO)_5/PhND_2$ and $H_2Os(CO)_4/PhND_2$ Isotope Exchange Reactions. Two CD_3CN solutions, one with [$HRe(CO)_5$] = 0.05 M and [$PhND_2$ (98% d)] = 0.76 M and the other with [$H_2Os(CO)_4$] = 0.05 M and [$PhND_2$ (98% d)] = 1.20 M, were prepared in NMR tubes and kept frozen at −196 °C up to the time of the experiment. The exchange reactions were monitored for more than 3 half-lives by NMR. The decrease in intensity of the metal hydride resonance was measured as a function of time. The slope of the line obtained from a plot of time versus ln [$A(t) - A(\infty)$], where $A(t)$ was the peak intensity at variable time

(35) Wailes, P. C.; Weigold, H.; Bell, A. P. *J. Organomet. Chem.* **1972**, *34*, 155.
(36) Coetzee, J. R.; Padmanabhan, G. R. *J. Am. Chem. Soc.* **1965**, *87*, 5005.
(37) Kolthoff, I. M.; Thomas, F. G. *J. Phys. Chem.* **1965**, *69*, 3049.
(38) Kolthoff, I. M.; Chantooni, M. K., Jr. *J. Am. Chem. Soc.* **1965**, *87*, 4428. This paper contains numerous references to previous incorrect measurements of the pK_a of picric acid in acetonitrile.

intervals and $A(\infty)$ was the peak intensity at $t = \infty$, was the observed first-order rate constant. Second-order rate constants were calculated by use of the appropriate form of the McKay equation (eq 12) and are listed in Table V.

Kinetics of the Reaction of Cp_2ZrMe_2 with $CpM(CO)_3H$ (M = W, Mo, Cr). Solutions of $CpM(CO)_3H$ and Cp_2ZrMe_2 in THF/0.5% benzene (or CD_3CN/0.5% benzene) were prepared and mixed under an inert atmosphere so that at least a tenfold excess (0.55-2.34 M) of the more plentiful reagent resulted (see Tables VI and VII). Because of the rapid reaction of Cp_2ZrMe_2 with $CpM(CO)_3H$ (M = Mo, Cr) in CD_3CN, it was necessary to add the solutions of these metal hydrides to a frozen solution of Cp_2ZrMe_2. All reaction mixtures were placed in NMR tubes, frozen and degassed several times, and then sealed under vacuum.

Kinetic runs at -6 °C and above were performed in constant temperature baths thermostatically controlled within ±0.1 or 0.2 °C. Samples were removed from the bath at appropriate intervals and quenched in liquid nitrogen. The NMR probe was cooled to 30 °C or more below the reaction temperature to prevent significant reaction while sampling. For reactions run at -6 °C or below, the reaction was run directly in the NMR probe. The sampling time corresponding to a particular point was then taken as the mean reaction time during the series of pulses required to collect that spectrum. In all cases the extent of reaction was determined by comparing peak heights of starting materials and products with that of an internal standard (benzene). Relative peak widths at half-height were routinely checked to ensure the validity of this procedure.

In most cases the peaks monitored were those of Cp ligands. However, when $CpCr(CO)_3H$ was a reactant, its Cp peak was broadened by the exchange of $CpCr(CO)_3^-$ units with the product. The extent of disappearance of $CpCr(CO)_3H$ was therefore determined from the decrease in height of its hydride peak. (The hydride chemical shift is unaffected by the exchange process and the hydride resonance therefore does not broaden.) In one case with near-equal concentrations of $CpCr(CO)_3H$ and Cp_2ZrMe_2 (the fourth run from the bottom in Table VII), the progress of the reaction was determined by monitoring the disappearance of Cp_2ZrMe_2.

The standard deviations of extrapolated rate constants were calculated from the standard deviations and covariance of $\Delta H^{\ddagger}$ and $\Delta S^{\ddagger}$.[1a]

Acknowledgment. This research was supported by NSF Grant CHE85-16415. We are grateful to Colonial Metals, Inc., for a donation of OsO_4, to Prof. Walter Klemperer for advice on measuring the rate of deprotonation of $HRe(CO)_5$, and to Prof. E. L. King for helpful discussions on the extraction of rate constants from the rate of approach to isotopic equilibrium.

Stereochemically Nonrigid Tungsten Alkylidene Complexes. Barriers to Rotation about the Tungsten to Carbon Double Bond

Jacky Kress and John A. Osborn*

Contribution from the Laboratoire de Chimie des Métaux de Transition et de Catalyse, U.A. au C.N.R.S. No. 424, Institut Le Bel, Université Louis Pasteur 4, 67000 Strasbourg, France.
Received August 27, 1986

Abstract: The tungsten alkylidene complexes $W(CHR)(OCH_2\text{-}t\text{-}Bu)_2Br_2$ [R = *n*-Bu (**4**), *sec*-Bu (**5**), Ph (**6**)], $W[\overline{C\text{-}(CH_2)_3CH_2}](OCH_2\text{-}t\text{-}Bu)_2Br_2$ (**7**), $W(CH\text{-}t\text{-}Bu)(OCH_2\text{-}t\text{-}Bu)_3X$ [X = Cl (**8**), Br (**9**), I (**10**)], $W(CHR)(OCH_2\text{-}t\text{-}Bu)_3Br$ [R = *n*-Bu (**11**), *sec*-Bu (**12**), Ph (**13**)], $W[\overline{C(CH_2)_3CH_2}](OCH_2\text{-}t\text{-}Bu)_3Br$ (**14**), and $W(CH\text{-}t\text{-}Bu)(OCH_2\text{-}t\text{-}Bu)_4$ (**15**) have been synthesized and studied by variable-temperature ^1H NMR spectroscopy. The low temperature limiting spectra observed for all these compounds (except for **15**) are consistent with a formal trigonal-bipyramidal arrangement of the five ligands around the tungsten. The carbene ligand occupies an equatorial position with its substituents lying in the trigonal plane. Notably the two diastereomers expected for **12** could be distinguished. At higher temperature, compounds **8**-**14**, but not compounds **4**-**7**, appear to undergo two distinct intramolecular dynamic processes. The lower energy process ($12.3 < \Delta G^{\ddagger} < 15.7$ kcal·mol^{-1}) consists of a simple carbene ligand rotation about the tungsten-carbon double bond. Its barrier is strongly dependent on the π-donor character of the ligands in the axial position of the bipyramid. Strong donors destabilize the ground state of these molecules by the resultant electronic repulsion created between the lone pairs of the π-donor ligand and the $(d_{xz}\text{-}p_z)$ π electrons of the metal-carbene π-bond. Since the orthogonal orientation of the carbene ligand is energetically largely unaffected by axial donation, the rotational barrier is thereby lowered. The higher energy process ($15.3 < \Delta G^{\ddagger} < 18.9$ kcal·mol^{-1}) consists of scrambling of all three neopentoxo groups, but it is not specific to carbene complexes. The particular behavior shown by compounds **15** and $[W(CH\text{-}t\text{-}Bu)(OCH_2\text{-}t\text{-}Bu)_3]^+Ga_2Br_7^-$ (**16**) is also discussed.

Transition-metal carbene complexes are generally recognized as important reactive intermediates in organometallic chemistry, in particular in certain catalytic reactions, e.g., olefin metathesis[1] and the Fischer-Tropsch synthesis.[2] The nature of the metal-carbon bonding interaction is thus of fundamental interest, and several theoretical studies have been carried out in attempts to evaluate its strength as well as the barrier to rotation about the expected metal-carbon double bond.[3] If structural studies on stable species show that metal-carbon bond lengths are effectively consistent with a double bonding interaction between the metal and the carbene fragment,[4] experimental studies on the rotational barrier are surprisingly limited in number, despite the numerous carbene complexes that have been synthesized in recent years. The only neutral high oxidation state complexes for which these barriers were determined experimentally are thus compounds MCp(CHR)X (M = Ta, Nb), in which the carbene-ligand rotation was found to be largely dependent on steric effects.[5]

Apart from these fundamental considerations, such barriers to carbene rotation, as well as the activation energies of other dynamic processes in carbene complexes, can have moreover important potential implications in chemical reactivity. For example,

(1) Ivin, K. J. *Olefin Metathesis*; Academic Press: London 1983.
(2) Muetterties, E. L. *J. Organomet. Chem.* **1980**, *200*, 177.
(3) (a) Lauer, J. W.; Hoffmann, R. *J. Am. Chem. Soc.* **1976**, *98*, 1729. (b) Schilling, B. E.; Hoffmann, R.; Lichtenberger, D. L. *Ibid.* **1979**, *101*, 585. (c) Rappé, A. K.; Goddard, W. A., III *Ibid.* **1980**, *102*, 5114. (d) Spangler, D.; Wendoloski, J. J.; Dupuis, M.; Chen, M. M. L.; Schaeffer, H. F., III *Ibid.* **1981**, *103*, 3987. (e) Nakamura, S.; Dedieu, A. *Nouv. J. Chim.* **1982**, *6*, 23. (f) Kostic, N. M.; Fenske, R. F. *J. Am. Chem. Soc.* **1982**, *104*, 3879. (g) Nakatsuji, H.; Ushio, J.; Han, S.; Yonezawa, T *Ibid.* **1983**, *105*, 426. (h) Taylor, T. E.; Hall, M. B. *Ibid.* **1984**, *106*, 1576. (i) Ushio, J.; Nakatsuji, H.; Yonezawa, T. *Ibid.* **1984**, *106*, 5892. (j) Marynick, D. S.; Kirkpatrick, C. M. *Ibid.* **1985**, *107*, 1993. (k) Gregory, A. R.; Mintz, E. A. *Ibid.* **1985**, *107*, 2179.
(4) See for instance: Casey, C. P.; Burkhardt, T. J.; Bunnell, C. A.; Calabrese, J. C. *J. Am. Chem. Soc.* **1977**, *99*, 2127. Churchill, M. R.; Missert, J. R.; Youngs, W. J. *Inorg. Chem.* **1981**, *20*, 3388.
(5) Schrock, R. R.; Messerle, L. W.; Wood, C. D.; Guggenberger, L. J. *J. Am. Chem. Soc.* **1978**, *100*, 3793.

0002-7863/87/1509-3953$01.50/0 © 1987 American Chemical Society